



Contents lists available at ScienceDirect

## Physica A

journal homepage: [www.elsevier.com/locate/physa](http://www.elsevier.com/locate/physa)

# Phase diagram of the mixed spin-2 and spin-5/2 Ising system with two different single-ion anisotropies



J.S. da Cruz Filho, M. Godoy\*, A.S. de Arruda

Instituto de Física, Universidade Federal de Mato Grosso, 78060-900, Cuiabá, Mato Grosso, Brazil

## HIGHLIGHTS

- Phase diagrams and compensation temperatures are examined for the mixed spin-2 and spin-5/2 Ising system with two single-ion anisotropies.
- The mean-field theory based on the Bogoliubov inequality for the Gibbs free energy is examined for the system.
- The Landau expansion of the free energy in the order parameter is obtained to describe the phase diagrams.
- The tricritical behavior is examined.

## ARTICLE INFO

### Article history:

Received 14 December 2012

Received in revised form 30 April 2013

Available online 22 August 2013

### Keywords:

Phase diagram

Single-ion anisotropies

Mean-field approximation

## ABSTRACT

We study the effect of two different single-ion anisotropies in the phase diagram and in the compensation temperature of mixed spin-2 and spin-5/2 Ising ferrimagnetic system. We employed the mean-field theory based on the Bogoliubov inequality for Gibbs free energy. We use the Landau expansion of free energy in the order parameter to describe the phase diagram. In the temperature versus single-ion anisotropy plane the phase diagram displays tricritical behavior. The critical and compensation temperatures increase with increasing values of the single-ion anisotropies.

© 2013 Elsevier B.V. All rights reserved.

## 1. Introduction

In the last five decades, the Ising model has been one of the most largely used models to describe critical behavior of several systems in nature. It is important to stress that in condensed matter theory it is relevant to describe the critical behavior and thermodynamic properties of a variety of physical systems (including disordered systems, spins glass, random field Ising systems, etc.). Recently, several extensions have been made in the spin-1/2 Ising model to describe a wide variety of systems. For example, the models consisting of mixed spins with different magnitudes are interesting extensions, forming the so-called mixed-spin Ising class.

Indeed, the discovery of molecular-based (MB) magnetic materials [1] has been one of the advances in modern magnetism. Many MB magnetic materials have two types of magnetic atoms regularly alternating which exhibit ferrimagnetism. In this context, a good description of their physical properties is given by means of mixed-spin configurations. Additionally, the interest in studying magnetic properties of molecular-based ferrimagnetic magnetic materials is due to their reduced translational symmetry rather than to their single-spin counterparts, since they consist of two interpenetrating sublattices. In this sense, Kaneyoshi et al. [2,3] have studied the magnetic properties as well as the influence of a single ion anisotropy in the compensation temperature ( $T$ ) of bipartite molecular-based ferrimagnet. They considered two problems, the first is that of a two-dimensional ferromagnetic Ising system composed of ferrimagnetically

\* Corresponding author. Tel.: +55 6536158734.

E-mail addresses: [zefilho@fisica.ufmt.br](mailto:zefilho@fisica.ufmt.br) (J.S. da Cruz Filho), [mgodoy@fisica.ufmt.br](mailto:mgodoy@fisica.ufmt.br) (M. Godoy), [aarruda@fisica.ufmt.br](mailto:aarruda@fisica.ufmt.br) (A.S. de Arruda).

ordered chains with alternating atoms of spin-1/2 and spin- $S$  ( $S > 1/2$ ) by using Ising spin identities and the differential operator technique. In the second case a diluted spin-2 and spin-5/2 ferrimagnetic Ising system was investigated on the basis of the effective-field theory with correlations. On other hand, Drillon et al. [4] analyze the thermodynamic behavior of an exchange-coupled linear system with two alternating spin sublattices, showing that a bimetallic complex chain like  $\text{MnNi}(\text{EDTA})6\text{H}_2\text{O}$  is a good example of an experimental realization of the mixed-spin system. Thus, ferrimagnetic materials are of great interest due to their possible technological applications and from a fundamental point of view. As discussed above, these materials are modeled by mixed-spin Ising model that can be built up by infinite combinations of different spins, where the pairs constituted by spins with values small are the simplest ((spin-1/2, spin-1), (spin-1/2, spin-3/2), (spin-1, spin-3/2), (spin-2, spin-3/2), (spin-2, spin-5/2), and so on).

Noteworthy, there are many studies on mixed-spin Ising systems aiming to explain the physical properties of disordered systems. This interesting topic has been a great challenge in statistical mechanics. In this regard, in the last years there has been great interest in the study of magnetic properties of systems formed by two sublattices with different spins and crystal field interactions [5]. One of the earliest and simplest type of these models was the mixed-spin Ising system consisting of spin-1/2 and spin- $S$  ( $S > 1/2$ ) in an uniaxial crystal field [6,7]. However, from a pure theoretical point of view, such systems have been widely studied by a variety of approaches, e.g., effective-field theory [8–17], mean-field approximation [18–20], renormalization-group technique [21], numerical simulation based on Monte-Carlo [22–32] and, finally, exact solutions for the mixed spin-1 and spin- $S$  Ising model in an uniaxial crystal field [33–38]. More recent interest is to extend such investigations into a more general mixed-spin Ising model with one constituent spin-1 and, in the simplest case, the other constituent spin-3/2. In this context, Abubrig et al. [39] presented a mean-field theory study to elucidate crystal field effects in the phase diagram of mixed spin-1 and spin-3/2 Ising configurations. Interestingly, they have found some outstanding new features in the  $T$ -dependence of both total and sublattice magnetizations.

In this paper, we study the effect of two different single-ion anisotropies in the phase diagram as well as in the compensation temperature of the mixed spin-2 and spin-5/2 Ising ferrimagnetic system. This case (the mixed spin-2 and spin-5/2 Ising ferrimagnetic system with two crystal-field interactions) primarily was studied on the Bethe lattice by using the exact recursion equations [40,41]. On the other hand, we employed the mean-field theory based on the Bogoliubov inequality for Gibbs free energy to describe the phase diagram. Thus, even knowing the limitation of the mean field theory, it is still an adequate starting point, and produces a very simple way to understand the possible critical behavior of physical systems. The paper is organized as follows: In Section 2, the model is introduced and analytical expressions for free-energy and equations of state are obtained. In addition, we derive the Landau expansion of free energy in the order parameter. In Section 3, we describe our theoretical results and discuss the phase diagram and the compensation temperature dependence. Finally, in Section 4 we present our conclusions.

## 2. The model and calculation

The mixed-spin ferrimagnetic Ising system consists of two interpenetrating square sublattices (A and B) with spin  $S^A = 0, \pm 1, \pm 2$  and spin  $S^B = \pm 1/2, \pm 3/2, \pm 5/2$ . In each site of the lattice there is a single-ion anisotropy ( $D_A$  in the sublattice A and  $D_B$  in the sublattice B) acting on the spins  $S = 2$  and spins  $S = 5/2$  at the lattice sites. The system is described by the following model Hamiltonian:

$$\mathcal{H} = -J \sum_{\langle i,j \rangle} S_i^A S_j^B - D_A \sum_{i \in A} (S_i^A)^2 - D_B \sum_{j \in B} (S_j^B)^2, \quad (1)$$

where the first term represents the interaction between the nearest neighbor spins at sites  $i, j$  located on sublattices A, B, respectively.  $J$  is the magnitude of the spin-spin interaction, and the sum is over all nearest neighbor pairs of spins. The second and third terms represent the single-ion anisotropies at all points of the sublattices A and B. The sums are performed over  $N/2$  spins of each sublattice.

In order to derive analytical expressions for free energy and equations of state, we employ the variational method based on the Bogoliubov inequality for Gibbs free energy [42], which reads

$$G(\mathcal{H}) \leq G_0(\mathcal{H}_0) + \langle \mathcal{H} - \mathcal{H}_0(\eta) \rangle_0 = \Phi(\eta). \quad (2)$$

Here,  $G(\mathcal{H})$  is the free energy of  $\mathcal{H}$ , and  $G_0(\mathcal{H}_0)$  is the free energy of a trial Hamiltonian  $\mathcal{H}_0(\eta)$  depending on variational parameters.  $\langle \cdot \cdot \cdot \rangle_0$  denotes a thermal average over the ensemble defined by  $\mathcal{H}_0(\eta)$ . To facilitate the calculations, we choose the simplest trial Hamiltonian, which is given by

$$\mathcal{H}_0 = - \sum_{i \in A} [D_A (S_i^A)^2 + \eta_A S_i^A] - \sum_{j \in B} [D_B (S_j^B)^2 + \eta_B S_j^B], \quad (3)$$

where  $\eta_A$  and  $\eta_B$  are variational parameters related to two different spins configurations. Within this approach we obtain the free energy and the equations of state (i.e., sublattice magnetization per site  $m_A$  and  $m_B$ ):

$$g = -\frac{1}{2\beta} \ln [2 \exp(4\beta D_A) \cosh(2\beta \eta_A) + 2 \exp(\beta D_A) \cosh(\beta \eta_A) + 1]$$

$$\begin{aligned}
 & -\frac{1}{2\beta} \ln \left[ 2 \exp\left(\frac{25}{4}\beta D_B\right) \cosh\left(\frac{5}{2}\beta \eta_B\right) + 2 \exp\left(\frac{9}{4}\beta D_B\right) \cosh\left(\frac{3}{2}\beta \eta_B\right) \right. \\
 & \left. + 2 \exp\left(\frac{1}{4}\beta D_B\right) \cosh\left(\frac{1}{2}\beta \eta_B\right) \right] - \frac{1}{2} J z m_A m_B + \frac{1}{2} \eta_A m_A + \frac{1}{2} \eta_B m_B,
 \end{aligned} \tag{4}$$

where  $\beta = 1/k_B T$ . The sublattice magnetizations per site  $m_A$  and  $m_B$  are defined by  $m_A = \langle S_i^A \rangle_0$  and  $m_B = \langle S_j^B \rangle_0$ , thus

$$m_A = \frac{2 \sinh(2\beta \eta_A) + \exp(-3\beta D_A) \sinh(\beta \eta_A)}{\cosh(2\beta \eta_A) + \exp(-3\beta D_A) \cosh(\beta \eta_A) + \frac{1}{2} \exp(-4\beta D_A)}, \tag{5}$$

and

$$m_B = \frac{1}{2} \left[ \frac{\exp(-6\beta D_B) \sinh\left(\frac{1}{2}\beta \eta_B\right) + 3 \exp(-4\beta D_B) \sinh\left(\frac{3}{2}\beta \eta_B\right) + 5 \sinh\left(\frac{5}{2}\beta \eta_B\right)}{\exp(-6\beta D_B) \cosh\left(\frac{1}{2}\beta \eta_B\right) + \exp(-4\beta D_B) \cosh\left(\frac{3}{2}\beta \eta_B\right) + \cosh\left(\frac{5}{2}\beta \eta_B\right)} \right]. \tag{6}$$

Minimizing the free energy in terms of the variational parameters  $\eta_A$  and  $\eta_B$ , we obtain

$$\eta_A = J z m_B \quad \eta_B = J z m_A, \tag{7}$$

where  $z$  is the coordination number. Hence, we find the generic mean-field equations (4)–(7), which provide the magnetic properties of our ferrimagnetic system. Since these Eqs. (5)–(7) have in general several solutions for the pair  $(m_A, m_B)$ , the stable phase will be the one which minimizes the free energy. The detailed phase diagram is determined numerically, but some features of the phase diagram can also be obtained analytically. Close to the second-order phase transition our solution can vary from an ordered state ( $m_A \neq 0$  and  $m_B \neq 0$ ) to a disordered state ( $m_A = 0$  and  $m_B = 0$ ). Given the fact that the magnetizations  $m_A$  and  $m_B$  are very small, we therefore expand the Eqs. (4)–(6) to obtain a Landau-like expansion:

$$g = A_0 + A_2 m_A^2 + A_4 m_A^4 + A_6 m_A^6 + \dots, \tag{8}$$

where the expansion coefficients are given by

$$A_0 = -\frac{1}{2\beta} \ln[(1 + y_a + x_a)(z_b + y_b + x_b)], \tag{9}$$

$$A_2 = \frac{1}{2\beta} \left[ \frac{t^2}{4} a_1 - \frac{t^2}{8} a_2 - \frac{t^4}{32} a_1^2 b_1 \right], \tag{10}$$

$$A_4 = \frac{1}{2\beta} \left[ \frac{t^4}{768} a_1^2 c_1 + \frac{t^3}{192} c_2 a_1 a_2 + \frac{t^2}{96} c_3 \right], \tag{11}$$

$$\begin{aligned}
 A_6 = \frac{1}{2\beta} & \left[ \frac{t^4}{11520} \left( c_4 + \frac{6}{t} c_5 \right) + t^5 \left( \frac{2a_2}{18423} c_2 (3a_1^2 - a_3) - \frac{c_5}{7680} a_2 a_1 \right) \right. \\
 & \left. + \frac{t^7 c_2}{18432} \left( a_4 - 3a_1^3 a_2^2 \right) + \frac{t^8}{245760} c_6 \right],
 \end{aligned} \tag{12}$$

with  $t = \beta J z$ , and

$$\begin{aligned}
 a_1 = \frac{z_{b_2} + 9z_{b_1} + 25}{z_{b_2} + z_{b_1} + 1}, \quad a_2 = \frac{4x_a + y_a}{x_a + y_a + 1}, \quad b_1 = \frac{25x_b + 9y_b + z_b}{x_b + y_b + z_b}, \\
 a_3 = \frac{z_{b_2} + 81z_{b_1} + 625}{z_{b_2} + z_{b_1} + 1}, \quad a_4 = \frac{16x_a + y_a}{x_a + y_a + 1}, \quad b_2 = \frac{625x_b + 81y_b + z_b}{x_b + y_b + z_b},
 \end{aligned} \tag{13}$$

$$a_5 = \frac{z_{b_2} + 729z_{b_1} + 15625}{z_{b_2} + z_{b_1} + 1}, \quad a_6 = \frac{64x_a + y_a}{x_a + y_a + 1}, \quad b_3 = \frac{15625x_b + 729y_b + z_b}{x_b + y_b + z_b}, \tag{14}$$

$$c_1 = \frac{t^4}{8} a_1^2 (3a_2^2 - a_4), \quad c_2 = \frac{t^3}{2} (3a_1^2 - a_3), \quad c_3 = \frac{t^2}{4} (3b_1^2 + 4a_3 - 12a_1^2 - b_2), \tag{15}$$

$$c_4 = \frac{t^2}{4} (-b_3 + 15b_1 b_2 - 30 - b_1), \quad c_5 = \frac{t^3}{4} (-15a_3 a_1 + a_5 + 30a_1^3), \tag{16}$$

$$c_6 = \frac{t^4}{12} (-a_6 a_1^6 - 30(a_2 a_1^2)^3 + 15a_2 a_4 a_1^6), \tag{17}$$

where

$$\begin{aligned}
 x_a = 2e^{4\beta D_A}; \quad y_a = 2e^{\beta D_A}; \quad z_{b_2} = e^{-6\beta D_B}; \quad z_{b_1} = e^{-4\beta D_B}, \\
 x_b = 2e^{\frac{25}{4}\beta D_B}; \quad y_b = 2e^{\frac{9}{4}\beta D_B}; \quad z_b = 2e^{\frac{1}{4}\beta D_B}; \quad t = z\beta.
 \end{aligned} \tag{18}$$

### 3. Results and discussions

The phase diagrams below are constructed according to the following routine: (i) numerical solutions for  $A_2 = 0$  and  $A_4 > 0$  provide second-order transition lines. (ii)  $A_2 = 0, A_4 = 0$  and  $A_6 > 0$  determine the tricritical points. (iii) The first-order transition lines are determined by comparing the corresponding Gibbs free energies of the various solutions of Eqs. (5) and (6) for the pair  $(m_A, m_B)$ . Moreover, we have also observed that  $A_6 > 0$  in the full  $T, D_A, D_B$  space. We also note that the coefficients  $A_2, A_4$  and  $A_6$ , in Landau expansion, are even functions of  $J$ , thus the critical behavior should be the same for both cases ferromagnetic ( $J > 0$ ) and ferrimagnetic ( $J < 0$ ).

For the particular case  $D_A = D_B = 0$ , the critical temperature is determined by taking  $m_A \rightarrow 0$  and  $m_B \rightarrow 0$ , or  $A_2 = 0$  and  $D_A = D_B = 0$ , giving  $k_B T_c / Jz = 2.4152$ . This value is qualitatively in agreement with estimates derived from effective-field theory with correlations (EFT) in the honeycomb lattice [3,5], and with the values of mean-field approximation (MFA) [3] for minor spins.

#### 3.1. The ground-state solution

The ground-state phase diagram (see Fig. 1) is determined from the Hamiltonian (1) by comparing the ground-state energies of different phases. At zero temperature, the structure of the ground state of our system consists of two disordered phases and six ordered phases with different values of  $\{m_A, m_B, q_A, q_B\}$ , corresponding to ordered ferrimagnetic phases:

$$O_1 = \left\{ -2, \frac{5}{2}, 4, \frac{25}{4} \right\}, \quad O_2 = \left\{ -2, \frac{3}{2}, 4, \frac{9}{4} \right\}, \quad O_3 = \left\{ -2, \frac{1}{2}, 4, \frac{1}{4} \right\},$$

$$O_4 = \left\{ -1, \frac{5}{2}, 1, \frac{25}{4} \right\}, \quad O_5 = \left\{ -1, \frac{3}{2}, 1, \frac{9}{4} \right\}, \quad O_6 = \left\{ -1, \frac{1}{2}, 1, \frac{1}{4} \right\},$$

and the disordered phases by

$$D_1 = \left\{ 0, \frac{5}{2}, 0, \frac{25}{4} \right\}, \quad D_2 = \left\{ 0, \frac{3}{2}, 0, \frac{9}{4} \right\},$$

where  $q_A = \langle (S_i^A)^2 \rangle$  and  $q_B = \langle (S_i^B)^2 \rangle$ . The energies are given by

$$E_1 = -\left( \frac{5}{2}Jz + 2D_A + \frac{25}{8}D_B \right), \quad E_2 = -\left( \frac{3}{2}Jz + \frac{1}{2}D_A + \frac{25}{8}D_B \right), \quad E_3 = -\left( \frac{1}{2}Jz + 2D_A + \frac{1}{8}D_B \right),$$

$$E_4 = -\left( \frac{5}{4}Jz + \frac{1}{2}D_A + \frac{25}{8}D_B \right), \quad E_5 = -\left( \frac{3}{4}Jz + \frac{1}{2}D_A + \frac{9}{8}D_B \right), \quad E_6 = -\left( \frac{1}{4}Jz + \frac{1}{2}D_A + \frac{1}{8}D_B \right).$$

#### 3.2. Phase diagram

The phase diagrams (Figs. 2 and 3) are analyzed in the  $(D_A/z|J|, k_B T/z|J|)$  and  $(D_B/z|J|, k_B T/z|J|)$  planes, where we follow the routine described at the beginning of this section.

In Fig. 2, we display the phase diagram of  $k_B T/z|J|$  versus  $D_A/z|J|$  for selected values of  $D_B/z|J|$ . At high temperatures, for all positive and negative values of  $D_B/z|J|$  within large range values of  $D_A/z|J|$ , the phase diagram shows only second-order phase transitions, which are indicated by solid lines. For values of  $D_B/z|J| > 2.5$ , all second-order lines end up in the same tricritical point given by  $(k_B T_t/z|J| = 1.1313, D_A/z|J| = -2.3300)$ . However, for values of  $D_B/z|J| < -2.5$  at low temperatures, all second-order lines end up at the same tricritical point given by  $(k_B T_c/z|J| = 0.2243, D_A/z|J| = -0.4667)$ . A heavy dotted curve connects these two tricritical points  $(k_B T_c/z|J| = 1.1313, D_A/z|J| = -2.3300)$  and  $(k_B T_t/z|J| = 0.2243, D_A/z|J| = -0.4667)$ . This curve separates the region with second and first-order phase transitions. In the low temperature regime and for all values of  $D_A/z|J|$  and  $D_B/z|J|$ , the phase transitions are found to be of first-order type. Thus, in this phase space  $(D_A/z|J|, k_B T/z|J|)$ , the system presents tricritical behavior. Additionally, the phase diagram shows that when  $D_B/z|J| \rightarrow +\infty$ , the mixed spin Ising system behaves like a two-level system since the spin-5/2 behaves like  $S^B = \pm 5/2$ . Nevertheless, in case that  $D_B/z|J| \rightarrow -\infty$ , the  $S^B = \pm 5/2$  states are suppressed and the system is equivalent to a mixed spin-1/2 and spin-2 Ising model. Thus, this is the reason why the coordinates of the tricritical point in the limit of large positive  $D_B/z|J|$  are higher than those for large negative  $D_B/z|J|$ . For the special case with equal anisotropic fields  $(D_A/z|J| = D_B/z|J| = 0)$  the critical temperature is  $k_B T_c/z|J| = 2.4152$ , and the location of the tricritical point is  $k_B T_t/z|J| = 0.8458, D_A/z|J| = -1.5537$ , for coordination number of lattice  $z$ .

In Fig. 3, we show the phase diagram of  $k_B T/z|J|$  versus  $D_B/z|J|$  for various values of  $D_A/z|J|$ . In the case of  $D_A/z|J| > -0.4716$  the phase transitions are only of second-order type (solid lines) for all values of  $D_B/z|J|$ . Here, the critical temperatures increase with  $D_B/z|J|$  and  $D_A/z|J|$ . Notice that in the range  $0.4716 > D_A/z|J| > -2.300$ , the phase

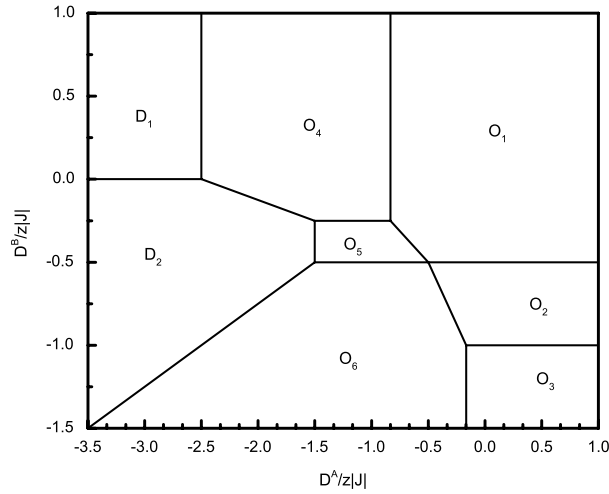


**Fig. 1.** Ground-state phase diagram of the mixed spin-2 and spin-5/2 Ising ferrimagnetic system with two different single-ion anisotropies  $D_A/z|J|$  and  $D_B/z|J|$ . The six ordered phases are represented by  $O_1 = \{-2, \frac{5}{2}, 4, \frac{25}{4}\}$ ,  $O_2 = \{-2, \frac{3}{2}, 4, \frac{9}{4}\}$ ,  $O_3 = \{-2, \frac{1}{2}, 4, \frac{1}{4}\}$ ,  $O_4 = \{-1, \frac{5}{2}, 1, \frac{25}{4}\}$ ,  $O_5 = \{-1, \frac{3}{2}, 1, \frac{9}{4}\}$ ,  $O_6 = \{-1, \frac{1}{2}, 1, \frac{1}{4}\}$ ,  $D_1 = \{0, \frac{5}{2}, 0, \frac{25}{4}\}$ ,  $D_2 = \{0, \frac{3}{2}, 0, \frac{9}{4}\}$ .

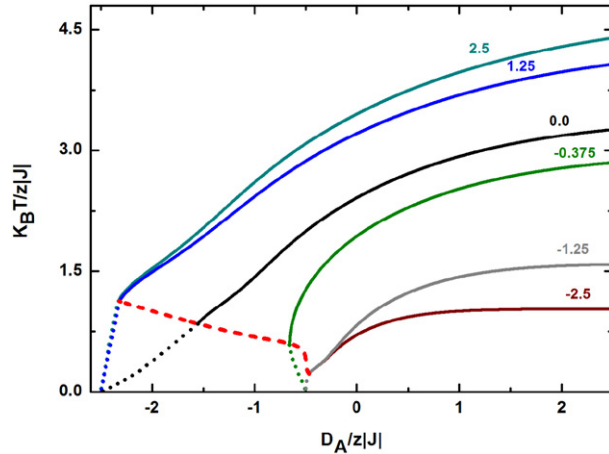


**Fig. 2.** Phase diagram in the  $(D_A/z|J|, k_B T/z|J|)$  plane for the mixed-spin Ising ferrimagnet with the coordination number  $z$ , for several values of  $D_B/z|J|$ . The solid and light dashed lines, respectively, indicate second- and first-order phase transitions, while the heavy dashed line represents the positions of tricritical points.

transitions are of second-order type in the high temperature region (solid lines) and of first-order (light dashed lines) at low temperatures. A heavy dotted curve of tricritical points separates the second- from the first-order transition lines.

One additional interesting feature shown in Fig. 3 refers to the fact that the phase transitions are only of first-order for  $|D_A/z|J| < -2.300$ . All lines that start below the heavy dotted line will necessarily be of first-order type. As seen, in this space  $(D_B/z|J|, k_B T/z|J|)$ , the system presents tricritical behavior.

These results may be compared to those obtained in Ref. [18], which apparently has a problem in their Eq. (4) and consequently in Eq. (8). These problems led to very different phase diagrams at finite temperatures.

### 3.3. Compensation temperature

The present mixed-spin system can exhibit compensation points. In order to clarify this property, we will consider the case of  $J < 0$ . The sign of the sublattice magnetizations are different since we are taking into account the fact that in the ferrimagnetic phase the system consists of two interpenetrating square sublattices (A and B) with spin-2 and spin-5/2. It is plausible that the magnetization of the sublattices cancel out at temperatures lower than the critical temperature. So, the total magnetization per site  $M = (m_A + m_B)/2$  is zero, in spite of the fact that  $m_A \neq 0$  and  $m_B \neq 0$ . This implies that we have compensation points in a characteristic temperature  $T_{\text{comp}}$  with  $T_{\text{comp}} < T_c$ . Fig. 4 shows the sublattice magnetizations  $m_A$  (dashed lines) and  $m_B$  (solid lines) for  $D_B = 0.0$  and  $T = 2.5$  (a),  $T = 2.25$  (b), and  $T = 2.0$  (c). The intersection between

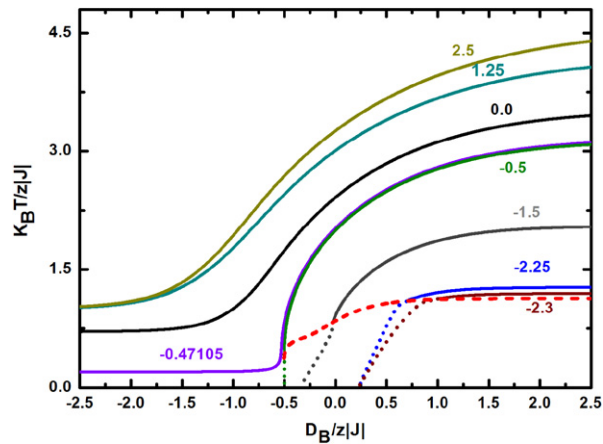


**Fig. 3.** Phase diagram in the  $(D_B/z|J|, k_B T/z|J|)$  plane for the mixed-spin Ising ferrimagnet with the coordination number  $z$ , for several values of  $D_A/z|J|$ . The solid and light dashed lines, respectively, indicate second- and first-order phase transitions, while the bold dashed line shows the positions of tricritical points.

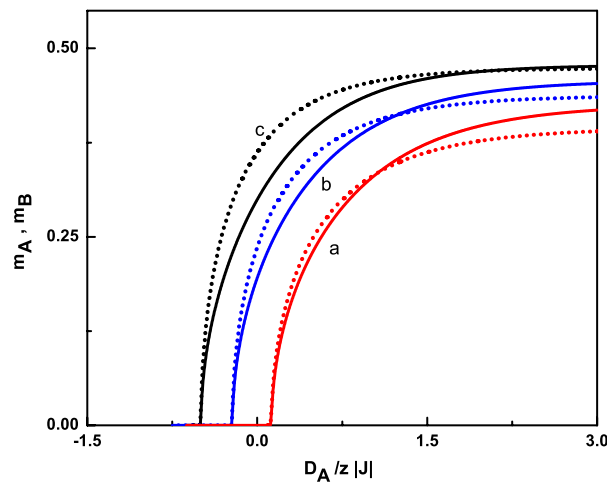


**Fig. 4.** The dependence of the sublattice magnetizations  $m_A$  (dashed lines) and  $m_B$  (solid lines) for  $D_B = 0.0$  and  $T = 2.5$  (a),  $T = 2.25$  (b), and  $T = 2.0$  (c).

the dashed and the solid line indicates the compensation point. At this point the total magnetization has zero value with sublattice magnetizations being different from zero ( $m_A \neq 0$  and  $m_B \neq 0$ ), as clearly seen in Fig. 4.

In Fig. 5, we present the diagram  $T_c$  and  $T_{\text{comp}}$  versus  $D_A/z|J|$  for selected values of  $D_B/z|J|$ . The diagram shows that there are compensation points in the range  $0.6335 > D_B/z|J| > -2.5$  and for  $D_A/z|J| > -0.625$ . Compensation points are indicated by dotted lines, while solid lines indicate the critical temperature. The inset in Fig. 5 exhibits some compensation points for  $D_B/z|J| = -2.5$ . On the other hand, the Fig. 6 exhibits the diagram  $T_c$  and  $T_{\text{comp}}$  versus  $D_B/z|J|$  for selected values of  $D_A/z|J|$ . This figure confirms our results shown in Fig. 5, i.e., there is a compensation temperature in the range between  $0.6335 > D_B/z|J| > -2.5$  and  $D_A/z|J| > -0.625$ .

#### 4. Conclusions

In summary, we have studied the effect of two different single ion anisotropies in the phase diagram and in the compensation temperature of the mixed spin-2 and spin-5/2 ferrimagnetic Ising system by using the mean field theory based on the Bogoliubov inequality. The phase diagrams are shown in the critical temperature versus single ion anisotropies plane. The system presents tricritical behavior, i.e., the second-order phase transition line is separated from the first-order transition line by a tricritical point. Additionally, we have also observed regions of compensation temperatures. Therefore, we predict that such a system may exhibit tricritical behavior and compensation temperatures due to the two different single ion anisotropies.

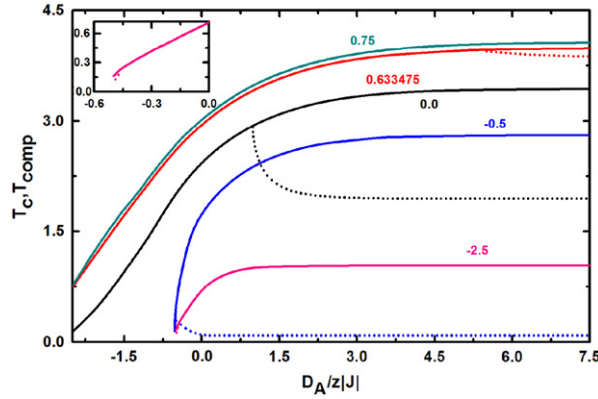


**Fig. 5.** The critical  $T_c$  and compensation  $T_{comp}$  temperatures as a function of the single-ion anisotropy  $D_A/|J|$ , and for different values of  $D_B/|J|$ . The solid and dotted curves represent the critical temperature and compensation temperature, respectively. The inset shows a magnification of the region where the compensation and critical temperatures are together for  $D_B/|J| = -0.625$ .

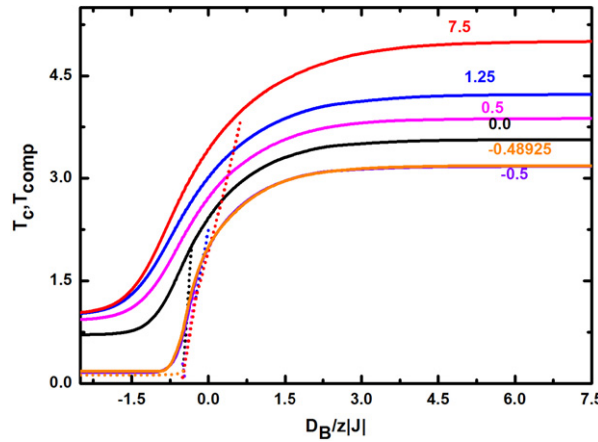


**Fig. 6.** The critical  $T_c$  and compensation  $T_{comp}$  temperatures as a function of the single-ion anisotropy  $D_B/|J|$ , and for several values of  $D_A/|J|$ . The solid and dotted curves represent the critical temperature and compensation temperature, respectively.

### Acknowledgments

Financial support from the Brazilian Agencies CAPES and FAPEMAT is gratefully acknowledged. The authors thank L. Craco for a careful reading of this manuscript and for making valuable suggestions to improve the quality of the presentation.

### References

- [1] O. Kahn, Molecular Magnetism, VCH, New York, 1993.
- [2] T. Kaneyoshi, Y. Nakamura, J. Phys.: Condens. Matter 10 (1998) 3003.
- [3] T. Kaneyoshi, Y. Nakamura, S. Shin, J. Phys.: Condens. Matter 10 (1998) 7025.
- [4] M. Drillon, E. Coronado, D. Beltran, R. Georges, J. Chem. Phys. 79 (1983) 449.
- [5] A. Bobák, Physica A 258 (1998) 140.
- [6] H.F. Verona de Resende, F.C. Sá Barreto, J.A. Plascak, Physica A 149A (1988) 606.
- [7] E. Albayrak, M. Keskin, J. Magn. Magn. Mater. 261 (2003) 196.
- [8] T. Kaneyoshi, J. Phys. Soc. Japan 56 (1987) 2675.
- [9] T. Kaneyoshi, Physica A 153 (1988) 556.
- [10] T. Kaneyoshi, J. Magn. Magn. Mater. 92 (1990) 59.
- [11] A. Benyoussef, A. El Kenz, T. Kaneyoshi, J. Magn. Magn. Mater. 131 (1994) 173.
- [12] A. Benyoussef, A. El Kenz, T. Kaneyoshi, J. Magn. Magn. Mater. 131 (1994) 179.
- [13] A. Bobák, M. Jurčičin, Physica A 240 (1997) 647.
- [14] D.C. de Oliveira, A.A.P. da Silva, D.F. de Albuquerque, A.S. de Arruda, Physica A 386 (2007) 205–211.
- [15] T. Kaneyoshi, M. Jurčičin, P. Tomczak, J. Phys.: Condens. Matter 4 (1992) L653.
- [16] T. Kaneyoshi, Physica A 205 (1994) 677.
- [17] D.F. de Albuquerque, S.R.L. Alves, A.S. de Arruda, Phys. Lett. A 346 (2005) 128–132.
- [18] H.K. Mohamad, E.P. Domashevskaya, A.F. Klinskikh, Physica A 388 (2009) 4713.
- [19] T. Kaneyoshi, J.C. Chen, J. Magn. Magn. Mater. 98 (1991) 201.

- [20] W.G. Zhu, M.H. Ling, *Commun. Theor. Phys.* 51 (2009) 756.
- [21] S.G.A. Quadros, S.R. Salinas, *Physica A* 206 (1994) 479.
- [22] G.M. Zhang, C.Z. Yang, *Phys. Rev. B* 48 (1993) 9452.
- [23] G.M. Buendia, M.A. Novotny, *J. Phys.: Condens. Matter* 9 (1997) 5951.
- [24] G.M. Buendia, J.A. Liendo, *J. Phys.: Condens. Matter* 9 (1997) 5439.
- [25] M. Godoy, W. Figueiredo, *Phys. Rev. E* 61 (2000) 218.
- [26] M. Godoy, W. Figueiredo, *Phys. Rev. E* 65 (2002) 026111.
- [27] M. Godoy, W. Figueiredo, *Phys. Rev. E* 66 (2002) 036131.
- [28] G. Wei, Q. Zhang, Y. Gu, *J. Magn. Magn. Mater.* 301 (2006) 245.
- [29] G. Wei, Y. Gu, Jing Liu, *Phys. Rev. B* 74 (2006) 024422.
- [30] M. Zukovič, A. Bobák, *Physica A* 389 (2010) 5401.
- [31] M. Zukovič, A. Bobák, *J. Magn. Magn. Mater.* 322 (2010) 2868.
- [32] R.A. Yessoufou, S. Bekhechi, F. Hontinfinde, *Eur. Phys. J. B* 81 (2011) 137.
- [33] L.L. Goncalves, *Phys. Scr.* 32 (1985) 248.
- [34] L.L. Goncalves, *Phys. Scr.* 33 (1986) 192.
- [35] J. Strečka, L. Čanová, M. Jaščur, *Phys. Rev. B* 76 (2007) 014413.
- [36] N.R. de Silva, S.R. Salinas, *Phys. Rev. B* 44 (1991) 852.
- [37] A. Dakhama, N. Benayad, *J. Magn. Magn. Mater.* 213 (2000) 117.
- [38] J.W. Tucker, *J. Magn. Magn. Mater.* 195 (1999) 733.
- [39] O.F. Abubrig, D. Horvath, A. Bobák, M. Jaščur, *Physica A* 296 (2001) 437.
- [40] A. Yigit, E. Albayrak, *J. Magn. Magn. Mater.* 309 (2007) 87.
- [41] A. Yigit, E. Albayrak, *Phys. Lett. A* 372 (2008) 361–366.
- [42] H. Falk, *Amer. J. Phys.* 38 (1970) 858.